

Influence of Temperature Gradient on Surface properties of Nitriding AISI 304 Stainless Steel

F. M. El-Hossary¹, N. Z. Negm¹, A. M. Abd El-Rahman^{2,1}, A. A. Abd El-Moula, S.M. Khalil^{1,3,4*}

¹Physics Department, Faculty of Science, Sohag University, 82524-Sohag, Egypt

²King Abdul-Aziz University, Jeddah, KSA.

³University College, Umm Al-Qura University, Alqunfadah, KSA.

⁴Umm Al-Qura University, Qunfadah Center for Scientific Research (QCSR), KSA

Abstract—AISI 304 austenitic substrates with different thicknesses were treated using rf plasma nitriding. This is to study the influence of the temperature gradient on the surface properties of the treated samples including nitrogen diffusivity and microstructure. X-ray diffraction, optical microscopy and scanning electron microscopy were used to characterize the treated samples. The results revealed that the surface temperature and temperature gradient of the nitrated substrate are substrate thickness dependent. It was found that the thickness of nitrated samples increases substantially as the temperature gradient increases from 1.93×10^5 to 10×10^{50} C/m. The microstructure is characterized mainly by the nitride phases of nitrogen expanded austenite (γ_N) and chromium nitride (CrN). Furthermore, the iron nitride phase of Fe_4N is detected at temperature gradient of 4.1×10^{50} C/m and lower. A maximum value of the nitriding rate of $1.21 \mu m^2/s$ have been observed with the temperature gradient of 10×10^{50} C/m.

Keywords—Temperature gradient, AISI 304 stainless steel, rf plasma nitriding, surface morphology.

1. Introduction

Austenitic stainless steels are commonly used in many industrial applications owing to their superior corrosion resistance. However, they demonstrate low surface hardness, poor tribological properties and low load-bearing capacity which limit some of their advanced applications when their resistance to plastic deformation is required. Therefore, surface treatment technology is applied to improve the mechanical and tribological properties; various nitriding processes have been widely used for several decades [1-8]. One of the best techniques is plasma nitriding owing to its good efficiency that can improve the surface properties of these alloys within shorter processing times with good surface finishing [8-10].

Intensive research work have been done on the effect of treatment temperature, processing time, processing power and, gas mixture even surface roughness on the surface properties of stainless steels [11-15]. The present work focuses on the influence of the temperature gradient on nitriding process. The temperature gradient is achieved by applying the technology on the AISI 304 austenitic

substrate with different thicknesses. The microstructure and surface morphology of the treated layers were investigated.

2. Experimental details

AISI 304 austenitic stainless steel substrates were cut into coupons with dimensions 20 mm x 15 mm with different thickness of (0.45, 0.65, 1.2, 1.45, 3 mm). The chemical composition of austenitic substrate is 0.5 wt.% Si, 1.2 wt.% Mn, 8.5 wt.% Ni, 19.1 wt.% Cr, 0.075 wt.% C and 69.95 wt.% Fe. The nitriding process was carried out using an inductively coupled rf plasma with a continuous mode of operation. The discharge was generated by a three-turn copper induction coil energized from a 13.56 MHz rf power supply through a tunable matching network. The sample is mainly heated using the only source of rf plasma field. The treatment temperature is measured during the rf plasma process by a Chromel–Alumel thermocouple, which was lightly pressed on the surface of the sample. The untreated samples were only cleaned in acetone before entering the reactor tube of the rf plasma system. To meet the optimum conditions of nitriding, the distance between the surface of the samples and rf coil was fixed at 21 mm. Nitrogen gas was introduced into the reactor tube to increase the base pressure from 7×10^{-3} to about 8×10^{-2} mbar. All samples were treated at a fixed input plasma processing power of 450 W for 10 min and the water flow rate was 1000 cm^3/min . At the end of the process, the nitrated sample was allowed in the evacuated atmosphere of nitrogen in the reactor tube until it cooled down to the room temperature.

In order to obtain a highly reflective surface of the nitrated layers for cross-section morphology investigation, the specimens should be carefully cut, grinded and exposed to subsequent polishing operations before they can be examined under optical microscope. Through this work, low speed saw of ISOMET™ is used for precise and deformation-free cutting of the treated specimens into small work pieces. Grinding was accomplished by abrading the specimen surface through a sequence of operations using progressively finer abrasive grit (silicon carbide) sizes from 40 mesh through 150 mesh were used as coarse abrasives, and grit sizes from 180 mesh through 400 mesh as fine abrasives. Polishing process was started by the abrasive grit of 600 and 1200 mesh. After that, the micro polish of Alumina suspensions (0.3 and 0.1 micron) was used on the top of the laps to achieve high quality polished surface mirror like. Finally, the specimens were washed and swabbed in warm running water. To show the morphology of the cross section of the treated samples, 2% nital etcher was used for exposure time of 30 s. Then, the layer thickness was measured by a micrometer scale attached

with the optical microscope and visibly confirmed by the optical images.

The microstructure of the nitrided layers was characterized by Philips x-ray Diffractometer using $\text{CuK}\alpha$ radiation ($\lambda = 1.540560 \text{ \AA}$). Optical microscope and scanning electron microscopy (SEM) were employed to study the surface microstructure of the nitrided substrates.

3. Results & Discussion

3.1 Surface temperature and temperature gradient

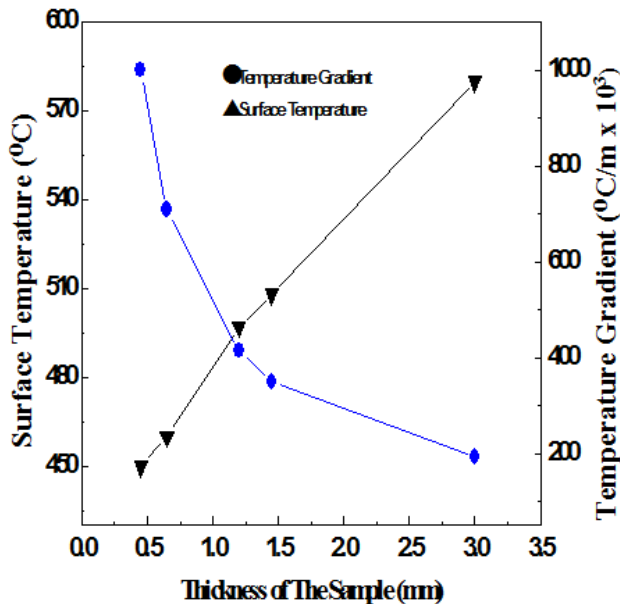


Fig. (1): The surface temperature and temperature gradient of nitrided austenitic stainless steel samples with different thicknesses.

Fig. 1 shows the surface temperature and temperature gradient of nitrided austenitic stainless steel substrates with different substrate thicknesses. One can observe that the surface temperature and temperature gradient are substrate thickness dependent. The surface temperature is continuously increased from 450 to 580°C with the increase of the substrate thickness from 0.45 to 3 mm. It has also found that the temperature gradient is decreased from 10×10^5 to 1.93×10^5 °C/m with the increase of the substrate thickness.

3.2 Microstructural Analysis

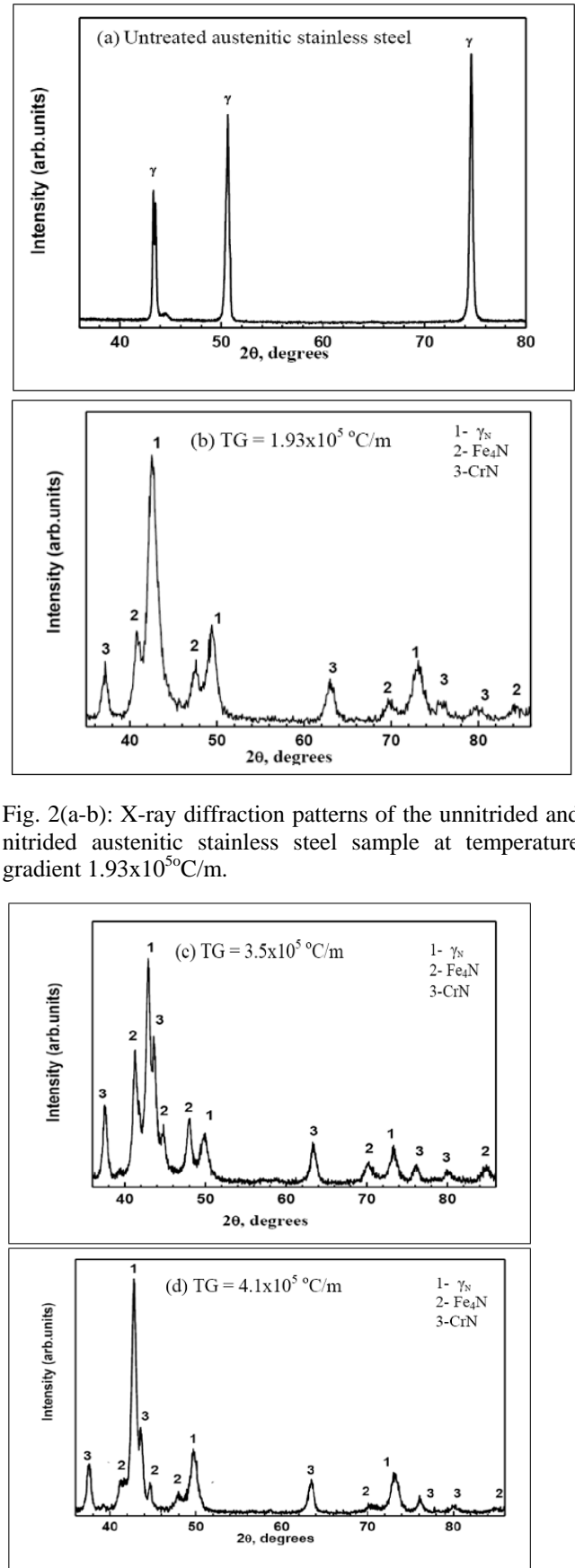


Fig. 2(a-b): X-ray diffraction patterns of the unnitrided and nitrided austenitic stainless steel sample at temperature gradient 1.93×10^5 °C/m.

Fig. 2(c-d): X-ray diffraction patterns of the nitrided austenitic stainless steel sample at temperature gradients 3.5×10^5 and 4.1×10^5 °C/m.

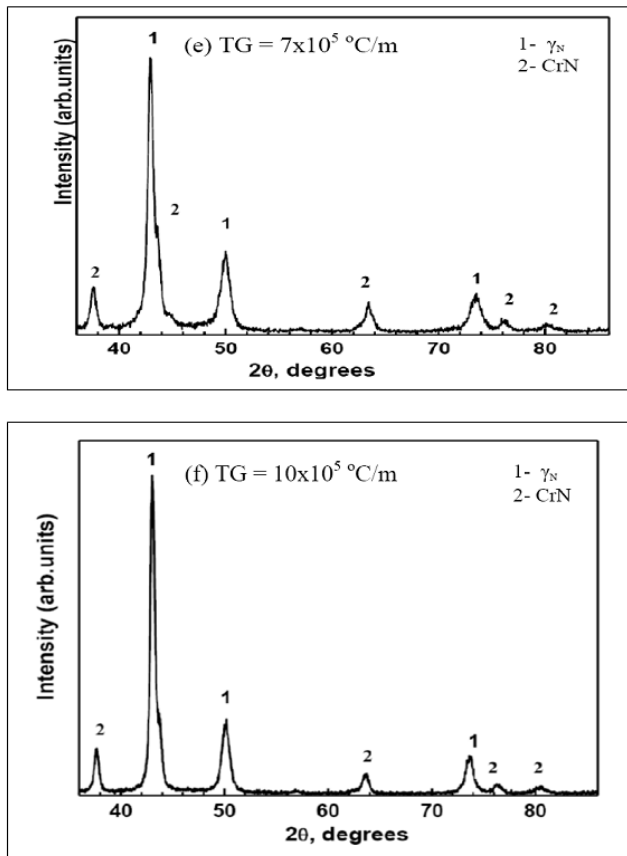


Fig. 2(e-f): X-ray diffraction patterns of the nitrided austenitic stainless steel sample at temperature gradients 7×10^5 and $10 \times 10^5 \text{ } ^\circ\text{C/m}$.

Fig. 2(a-f) shows the XRD spectrum of the untreated and treated austenitic stainless steel samples at different temperature gradients. A typical pattern of the untreated sample is examined and shown here for comparison in (Fig. 2-a). This figure reveals that all intense peaks are assigned to the austenitic stainless steel γ -phase. The treated samples demonstrate different microstructures with varying of the temperature gradient. Their microstructure is characterized mainly by solid solution phase of nitrogen expanded austenite phase (γ_N) and chemical compound phase of chromium nitride (CrN) while; the peaks of γ -phase diminish. Furthermore, iron nitride phase of Fe_4N is detected at temperature gradient of $4.14 \times 10^5 \text{ } ^\circ\text{C/m}$ and lower. However, the treated samples at temperature gradient of $7.1 \times 10^5 \text{ } ^\circ\text{C/m}$ and higher show the presence of γ_N and CrN without the formation of Fe_4N . Typical microstructure has been observed in the nitrided austenitic stainless steels while the treatment temperature was maintained at $450 \text{ } ^\circ\text{C}$ [16]. From this figure, it is evident that the relative intensity of Fe_4N and CrN increases with decreasing the temperature gradient.

It is worth mentioning that the diffraction peaks of nitrogen expanded austenitic stainless steel shift towards lower angles compared to that of unstrained austenitic substrate. This shift is found to be limited to approximately $1.3 \pm 0.6 \%$ due to the formation of chemical compounds of CrN and Fe_4N which affect the amount of nitrogen species inserted into the expanded austenitic stainless steel. The dependence of lattice expansion on the concentration of

nitrogen has been previously studied and has been found that the more nitrogen concentration the higher lattice expansion [17].

3.3 Cross- Section morphological analysis

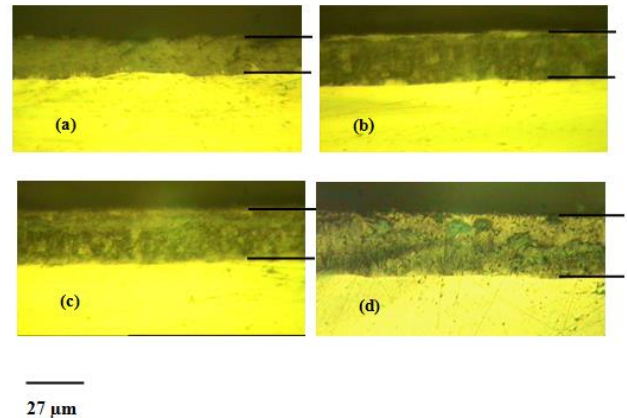


Fig. (3): Cross section optical microscope of nitrided sample at temperature gradients (a) 1.9×10^5 , (b) 3.5×10^5 (c) 7.1×10^5 and (d) $10 \times 10^5 \text{ } ^\circ\text{C/m}$

Fig. 3(a-d) shows typical optical micrographs of the cross-section of the nitrided samples at different temperature gradients. The nitrided layer for all treated samples reveals a homogeneous band and a sharp interface with the bulk material. The modified layer may be attributed to promotion of nitrogen ionization, leading to high concentration of high-energy ions supplied on to the specimen. Similar results have been observed for nitriding stainless steel using different plasma techniques [18].

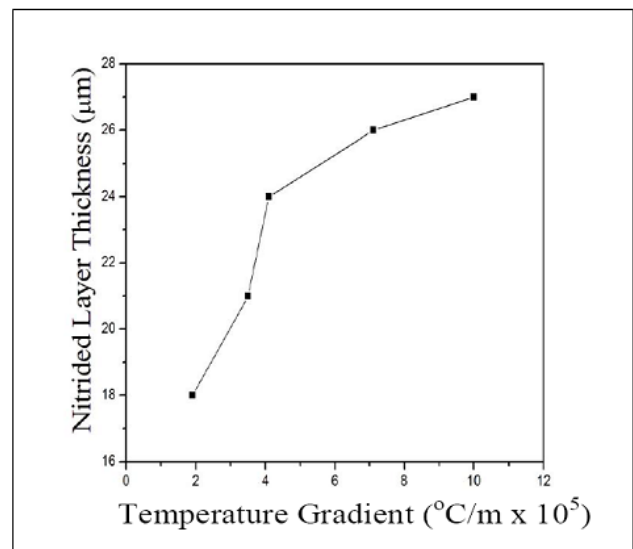


Fig. (4): Nitrided Layer Thickness and temperature gradient of nitrided austenitic stainless steel samples.

It has been found that the thickness of the nitrided layer increases as the temperature gradient increases substantially as seen in fig. 4. The enhancement of thickness is probably due to acceleration of nitrogen diffusion by the action of temperature gradient. This nitrided layer provides a path of rapid nitrogen transportation in the material. This leads to the conclusion that, the

temperature gradient play a more dramatic role on thickness of compound layer.

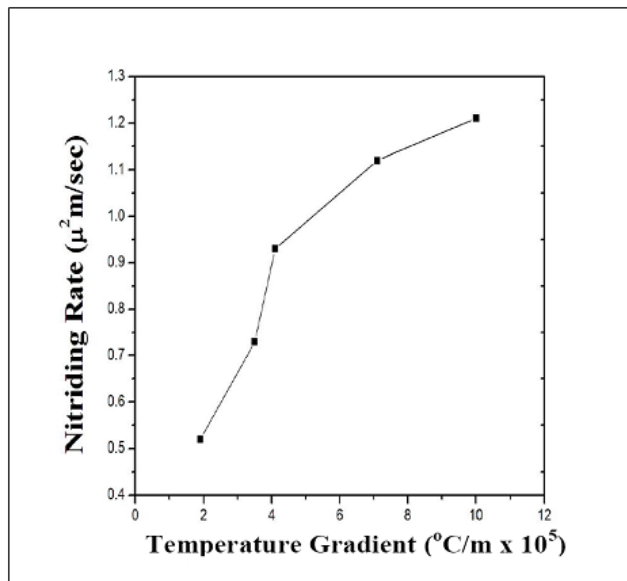


Fig. (5): Nitriding Rate and temperature gradient of nitrided austenitic stainless steel samples.

Fig. 5 displays nitriding rate variation as a function of the temperature gradient, from this figure; it can be observed that the nitriding rate increases as the temperature gradient increases. The nitriding efficiency and the microstructure of the nitrided layer can be affected by temperature gradient and surface temperature. The temperature gradient affects mainly the diffusion process. The inward diffusion of nitrogen species takes the same direction of heat transfer towards the bulk substrate. The continuous increase of the nitriding rate could be ascribed to the increase of the temperature gradient which enhances the diffusion process of reactive nitrogen species toward the bulk substrate.

The anomalously nitriding rate can be interpreted according to the mechanism of concentration gradient and the role of microcracks which could be numerous grown on the surface during the nitriding process at optimized plasma parameters [19-20]. In the initial stage of the nitriding process, high energetic plasma species created out at plasma processing power of 450 W was found to be efficient to remove most of the native oxide layer. In parallel to this, more microcracks can be formed; offering a high opportunity for more chemical reactions on the nitrided surface. These surface defects work as highly active channels to enhance the diffusion process of nitrogen species toward the bulk material. However, the nitriding rate variation might be attributed to temperature gradient and the internal stress created by the nitrided phases. The present study displays that the diffusion of plasma species inward the bulk substrate is relatively restricted at low temperature gradient compared to high temperature gradient. From the above, it can be concluded that the temperature gradient has a positive effect on the nitriding rate.

Furthermore, the surface temperature affects mainly the microcracks (number and size) formed on the surface of the austenitic substrate which works as channels

for the diffusion of the reactive plasma species inward the bulk material [20]. Therefore, the surface temperature can be considered as another contributing factor, affects the nitriding rate.

3.4 Surface morphology

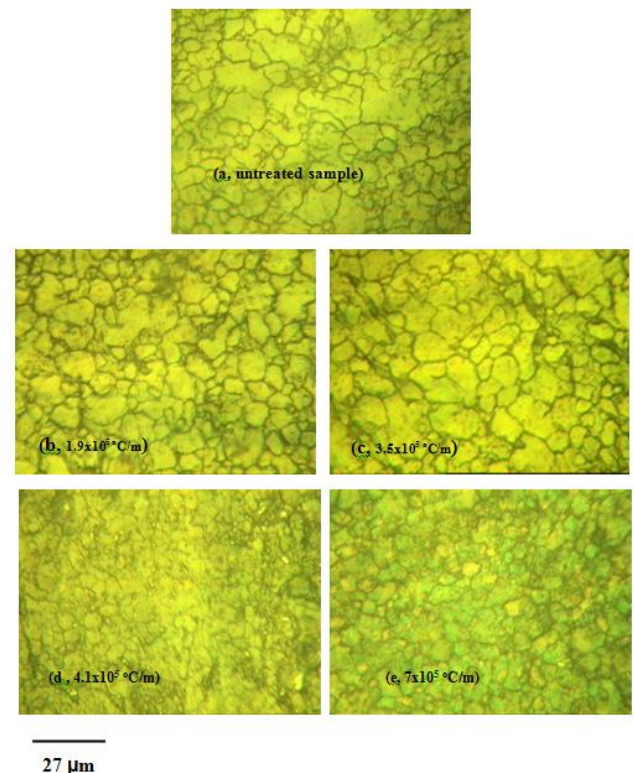


Fig. (6): Surface morphology of the untreated (a) and treated austenitic stainless steel sample at temperature gradients (b) 1.9×10^5 , (c) 3.5×10^5 (d) 4.1×10^5 and (e) 7×10^5 $^{\circ}\text{C/m}$.

Figure 6(a-e) shows the surface morphology of the untreated and treated austenitic stainless steel samples at different temperature gradients. As one can see from Fig. 6(a) the untreated sample appears that, surface discloses large, non-uniform and randomly packed grains with thin boundaries. Furthermore, undistributed micro-porous have been found on the surface. Fig. 6(b,c) shows that the nitrided samples at temperature gradient of 1.93×10^5 and 3.5×10^5 $^{\circ}\text{C/m}$. This figure reveals that slightly change in their microstructure with irregular grains due to the formation of multi-nitrided phases after surface treatment process [21]. The samples at temperature gradient of 4.14×10^5 $^{\circ}\text{C/m}$ and higher reveal a microstructure with smaller grain size separated with relatively thin grain boundaries compared to that observed in the microstructure of above samples. This microstructure as a result of the increased nitrogen solubility and diffusivity. Moreover, the dark precipitation of chromium nitride is observed for all treated samples. This observation agrees with Randall et al. [21] and abd El-Rahman et al. [22].

4. Conclusion

The present study displays that, the substrate thickness was increased with the increase of the temperature gradient. The diffusion process of nitrogen species inward the bulk substrate and other surface properties were found to be temperature gradient dependent. A maximum nitriding rate of approximately 1.2

$\mu\text{m}^2/\text{s}$ was achieved at a temperature gradient of 10×10^5 $^\circ\text{C}/\text{m}$. The substrates which nitrided at high temperature gradient from 4.1×10^5 $^\circ\text{C}/\text{m}$ and higher revealed a microstructure with smaller grain size separated with relatively thin grain boundaries compared to that observed in the microstructure of substrates nitrided at low temperature gradient regions from 3.5×10^5 $^\circ\text{C}/\text{m}$ and lower. This demonstrates grain size and grain boundaries strengthening mechanisms beside the variation of the microstructure which interpret the increase of the nitriding rate as a function of temperature gradient.

REFERENCES

- [1] J. Flis, J. Mankowski, E. Rolinski, Surf. Eng. 5 (2) (1989) 151.
- [2] Masato Sahara, Takayasu Sato, Shigeru Ito, Kazuo Akashi, Mater.Chem.Phys. 54 (1998) 123.
- [3] S. Kumar, M.J. Baldwin, M.P. Fewell, S.C. Haydon, K.T. Short, G.A.Collins, J. Tendys, Surf. Coat. Technol. 123 (2000) 29.
- [4] C. Muratore, D. Leonhardt, S.G.Walton, D.D. Blackwell, R.F. Fernsler, R.A. Meger, Surf. Coat. Technol. 191 (2005) 255.
- [5] V. Singh, K. Marchev, C.V. Cooper, E.I. Meletis, Surf. Coat. Technol. 160(2002) 249.
- [6] M.J. Baldwin, G.A. Collins, M.P. Fewell, S.C. Kumars, K.T. Short, J.Tendys, Jpn. J. Appl. Phys. 36 (7B) (1997 (Jul.)) 4941.
- [7] M.K. Lei, Y. Huang, Z.L. Zhang, J. Mater. Sci. Lett. 17 (1998) 1165.
- [8] F.M. El-Hossary, F. Mohammed, A. Hendry, D.J. Fabian, Z. Szazne-Csih, Surf. Eng. 4 (2) (1988) 150.
- [9] B. Edenhofer, Heat Treat. Met. 1 (1974) 23.
- [10] F. El-Hossary, J. Mater. Sci. Lett. 11 (1992) 1375.
- [11] L.C.Gontijo, Machado R., Miola E.J., Casteletti L.C., Alcântara N.G., and Nascente P.A.P., 2006 , Mater Sci. Eng. A, 431, 315.
- [12] Liang Wang, Shijun Ji, and Juncai Sun, 2006, Surf. Coat. Technol., 200, 5067.
- [13] EL-Hossary F. M., 2002, Surf. Coat. Technol., **150**, 277.
- [14] Lepienski C.M., Nascimento F.C., Foerster C.E., da Silva S.L.R., de M. Siqueira C.J.,and Alves Jr. C., 2008, Mater Sci. Eng. A, 489, 201.
- [15]Singh G.P., Alphonsa J., Barhai P.K., Rayjada P.A., Raole P.M., and Mukherjee S., 2006, Surf. Coat. Technol., **200**, 5807.
- [16]Larisch B., Brusky U., and Spies H.-J., 1999, Surf. Coat. Technol., **116-119**, 205.
- [17]Picard S., Memet J.B., Sabot R. , Grosseau-Poussard J.L., Rivière J.P., and Meilland R., 2001, Mater Sci. Eng. A, **303**, 163.
- [18] Mahfujur Rahman, Julfikar Haider, M.S.J. Hashmi, 2005, Surf. Coat. Technol., **200**, 1645.
- [19] EL-Hossary F. M., 2002, Surf. Coat. Technol., **150**, 277.
- [20]Pranevicius L.L., Valatkevicius P., Valincius V., Templier C., Riviere J.-P., and Pranevicius L., 2002, Surf. Coat. Technol., **156**, 219.
- [21] Randall N.X., Renevier N., Michel H., and Collignon P., 1997, Vacuum, 48, 849.
- [22]Abd El-Rahman A. M., Negm N. Z., Prokert F., El-Hossary F. M., Richter E., and Möller W., 2005, Surf. Coat. Technol., **191**, 140.